Available online at www.sciencedirect.com
ScienceDirect
Journal of the European Ceramic Society 29 (2009) 2885–2891
www.elsevier.com/locate/jeurceramsoc

Intercalation of Al into *M*C (*M* = Ti, V, Cr)

Denis Music *, Helmut Kölpin, Moritz to Baben, Jochen M. Schneider

Materials Chemistry, RWTH Aachen University, D-52056 Aachen, Germany

Received 9 December 2008; received in revised form 19 March 2009; accepted 30 March 2009
Available online 29 April 2009

Abstract

The energetics of point defects and twins in MC_x ($x<1$, M = Ti, V, Cr, space group $Fm\bar{3}m$) was studied using density functional theory. Our goal is to contribute towards understanding the underlying atomic mechanisms enabling the Al intercalation into MC_x. As the valence electron concentration is increased by substituting Ti in TiC_x with V and further with Cr, the energy of formation for C vacancies is decreased. This may be understood based on the electronic structure. Upon increasing the valence electron concentration, the bonding becomes less ionic and more covalent. In covalent crystals, directional bonding may be rearranged and local relaxation is observed upon vacancy creation, while this gives rise to repulsive Coulomb forces in ionic crystals, and hence the energy of formation is expected to decrease as the valence electron concentration of M is increased. The difference between the energy of formation for an Al substitution at a C site and a C vacancy, the migration energy for Al, the point defect ordering energy, and the twin boundary energy may be overcome, for instance, during vapor phase condensation. These results may be of general relevance for the formation of MAX phases (space group $P6_3/mmc$) at low temperatures.

Keywords: Carbides; Defects; Density functional theory

1. Introduction

Transition metal carbides exhibit many striking properties. They are known to be refractory solids,[1] possess large stiffness[2–4] and relatively low chemical reactivity,[1] as well as they are good thermal conductors.[5] However, the intrinsic brittleness is limiting their application potential.[6] The design of transition metal carbide/metal composites is one possibility to address the brittleness challenge.[7] In conch shells[8] and lobster cuticles,[9] biomineral composites of hard and soft phases may result in ductility and the arrest of cracks. The discovery of the so-called $M_{n+1}AX_n$ phases (space group $P6_3/mmc$), where layers of transition metal carbides or nitrides ($M_{n+1}X_n$) are interleaved with A-layers (mostly IIIA and IVA elements, such as Al or Si),[10–12] also provides a way to address the brittleness challenge discussed above. Owing to this particular nanolaminated atomic arrangement, these ternary derivatives of transition metal carbides or nitrides exhibit a combination of metallic and ceramic properties, ranging from machinability, large stiffness, good conductivity of heat and electricity, and good thermal shock resistance, to good corrosion resistance.[10]

A seemingly natural pathway to form these ternary phases is intercalation, for instance known to be successful for graphite.[13,14] In a recent study, this pathway has been utilized by Riley and Kisi[15] and they have demonstrated that Ti_3AlC_2 can be synthesized by the rapid intercalation of Al into $TiC_{0.67}$ (space group $Fm\bar{3}m$). The notion that $M_{n+1}AX_n$ phases can be formed by intercalating A-group elements into $M_{n+1}X_n$ has been introduced by Zhou and coworkers.[16,17] Riley and Kisi have suggested that, after the ingress of molten Al into $TiC_{0.67}$, vacancy ordering facilitates the formation of Ti_3AlC_2.[15] Similar pathways might be viable for the formation of Ti_3SiC_2 as well.[18] In a previous work,[19] we have studied the energetics of point defects at a C site in TiC_x ($x<1$): C vacancies and Al substitution at a C site. We have found minute energy differences for incorporation of Al at a vacant C site.[19] Our data indicate that Ti_3AlC_2 is formed by Al surface ingress into TiC_x and C vacancy ordering.[19] Furthermore, it is also known that both Al and Si promote twinning in TiC_x, which is another prerequisite to form $M_{n+1}AX_n$ phases.[20] The ability to form twins and the relevance thereof for the formation of $M_{n+1}AX_n$ phases has not been considered theoretically. Furthermore, there is no systematic study

* Corresponding author. Tel.: +49 2418025972; fax: +49 2418022295.
E-mail address: music@mch.rwth-aachen.de (D. Music).

0955-2219/$ – see front matter © 2009 Elsevier Ltd. All rights reserved.
doi:10.1016/j.jeurceramsoc.2009.03.030

available in literature exploring theoretically the possibility to form other $M_{n+1}AX_n$ phases than Ti_3AlC_2 by intercalation.

In this work, we study the energetics of point defects and twins in MC_x ($x<1$, M = Ti, V, Cr, space group $Fm\bar{3}m$) using *ab initio* calculations. In particular, we evaluate C vacancies, Al substitution at a C site, ordering of C vacancies with and without Al, migration of Al in the MC_x lattice, as well as twin boundary energy with and without Al. Our ambition is to contribute towards understanding the underlying atomic mechanisms enabling the Al intercalation into MC_x. We show that the difference between the energy of formation for an Al substitution at a C site and a C vacancy in bulk MC_x and on MC_x(1 0 0), the migration energy, the point defect ordering energy, and the twin boundary energy may be overcome, for example, during vapor phase condensation. Based on this study, it is reasonable to assume that intercalation of Al into MC_x (M = V, Cr) is realizable.

2. Theoretical methods

Density functional theory was used herein,[21] as implemented in the Vienna *ab initio* simulation package (VASP), where the projector augmented wave potentials with the generalized-gradient approximation are employed.[22] The following settings were employed: the total energy convergence criterion of 0.01 meV, Blöchl corrections for the total energy,[23] a cut-off of 500 eV, and integration in the Brillouin zone according to Monkhorst-Pack[24] with 262144 grid points in the FFT-mesh. Spin polarization was tested for CrC and only negligible energy corrections were found. MC $2\times2\times2$ supercells, built of 64 atoms, were relaxed with respect to atomic positions and cell volumes. Since there were no local structural relaxations beyond the second coordination shell, the calculations were found reliable with respect to the supercell size.[19] Vacancies and Al substitutions were always considered at C sites, except for the twinning energy studies where Al substituted M elements as suggested previously,[20] which resulted in the following compositions: MC_x (x = 0.97 for single C vacancy, 0.91 for triple C vacancy, 0.97 and 0.91 for Al substitution, 0.94 for migration, 1.00 and 1.33 for twinning). It is also known that Al may substitute M elements in these binary carbides.[25,26] However, according to Riley and Kisi[15] C vacancies are required to form $M_{n+1}AX_n$ phases by Al substitutions on C sites. Bulk moduli were obtained by fitting the energy-volume curves using the Birch-Murnaghan equation of states.[27] Two different reference points were used to evaluate the point defect data: isolated atoms[28] and chemical potentials.[28–30] Energy of formation (E_V or E_S) for the vacancy or Al substitution at a C site, respectively, was calculated as follows:

$$E_V = \frac{E_{MC,V(C)} + nE_C - E_{MC}}{n}$$
$$E_S = \frac{E_{MC,S(Al)} + nE_C - E_{Al} - E_{MC}}{n} \quad (1)$$

where $E_{MC,V(C)}$, E_C, E_{MC}, $E_{MC,S(Al)}$, and E_{Al} are the total energy of MC with n C vacancies, the total energy of isolated C (broken periodic boundary conditions) or its chemical potential (space group $Fd\bar{3}m$), the total energy of the defect-free MC, the total energy of MC with an Al substitution at a C site, and the total energy of isolated Al (broken periodic boundary conditions) or its chemical potential (space group $Fm\bar{3}m$), respectively. This method was used for dealing with the energetics of both bulk and surface point defects. Migration energy for Al in [1 1 0] direction was also calculated. There are several possible pathways for Al to move to a neighboring vacant site and a saddle point was identified in our previous work.[19] The migration energy was calculated by evaluating the energy difference between the displaced Al and the supercell with Al at its ideal site. In this procedure, Al was always quenched at its displaced position while all other atoms were fully relaxed. Twin boundary energy (E_T) was obtained as follows:

$$E_T = \frac{E_{MC,T} - E_{MC}}{2A}, \quad (2)$$

where $E_{MC,T}$ and A designate the total energy of the MC crystal containing two twin boundaries and area of the twin, respectively. For the twin boundary energy determination, supercells containing 16 atoms were used, as previously introduced by Yu et al.[20] The electronic structure was studied by evaluating electron density distributions[31] and effective charges.[32] The effective charge was calculated for MC unit cells by the Bader charge analysis applying the Henkelman code.[33,34] Core charges were added to the electron density distribution to verify the Bader regions.

3. Results and discussion

3.1. Structure and elastic properties

Table 1 contains the calculated data of the lattice parameters, the bulk moduli, the energy of formation for the point defects, the migration energy, and the twin boundary energy for MC_x (M = Ti, V, Cr). The following bulk configurations were considered: (i) one C vacancy, (ii) three C vacancies dispersed in the MC_x lattice [(0,0,0), (1/4,3/4,0), (1/4,1/4,1/2)], (iii) three C vacancies ordered along the [1 1 0] direction [(0,0,0), (1/4,1/4,0), (1/2,1/2,0)], (iv) one Al substitution at a C site, (v) two C vacancies and one Al substitution dispersed in the MC_x lattice [Al at (0,0,0), vacancies at (1/4,3/4,0), (1/4,1/4,1/2)], (vi) two C vacancies and one Al substitution ordered along the [1 1 0] direction [Al at (0,0,0), vacancies at (1/4,1/4,0), (1/2,1/2,0)], (vii) twins in pure MC_x, and (viii) twins in MC_x with Al placed at the twin boundary. The migration energy for Al at the (0,0,0) site was calculated in the [1 1 0] direction. Finally, the following (1 0 0) surface configurations were examined: (i) one C surface vacancy and (ii) one Al substitution at a C surface site. The calculated lattice parameter for pure TiC, VC, and CrC differs by 0.2%, −0.3%, and 1.0%, respectively, from the experimental data,[35–37] which is in good agreement. Upon introducing point defects, the lattice parameter decreases for vacancies and increases for Al substitution, which is consistent with literature.[36–39] The calculated bulk modulus for pure TiC is 12.1% larger than the experimentally obtained value,[38] which is within the expected deviation for the exchange-correlation approximation used here. Minor changes in the bulk moduli are observed when C vacan-

Table 1
Calculated lattice parameters (a), bulk moduli (B), energy of formation for the C vacancy (E_V), energy of formation for Al substitution at a C site (E_S), migration energy (E_M), and twin boundary energy (E_T) for MC (M = Ti, V, Cr). The data in parenthesis refer to surfaces. Two different reference points were used to evaluate the point defect data: isolated atoms (i) and chemical potentials (c).

	TiC	VC	CrC
a (Å)	4.338[a]	4.158	4.072
B (GPa)	265[a]	315	335
E_V (eV/defect)			
Single (i)	9.916 (9.763)[a]	8.450 (9.081)	7.713 (6.835)
Single (c)	0.827 (0.674)	−0.638 (−0.008)	−1.375 (−2.253)
Ordered (i)	10.072[a]	8.829	7.953
Ordered (c)	0.983	−0.260	−1.135
Disordered (i)	10.023[a]	8.633	7.723
Disordered (c)	0.935	−0.455	−1.365
E_S (eV/defect)			
Single (i)	10.140 (6.984)[a]	9.350 (6.276)	7.756 (4.369)
Single (c)	4.658 (1.502)	3.868 (0.794)	2.274 (−1.113)
Ordered (i)	10.110	4.986	10.304
Ordered (c)	5.253	0.129	5.447
Disordered (i)	10.029	4.787	10.093
Disordered (c)	5.173	−0.070	5.236
E_M (eV/defect)	0.820	0.573	0.479
E_T (J/m^2)			
Pure MC	0.929	0.494	0.026
MC with Al	−0.709	0.305	0.505

[a] Ref. 19.

cies or an Al substitution are introduced into TiC. To the best of our knowledge, there are no experimentally obtained bulk modulus data for pure VC or CrC. For $VC_{0.85}$, the experimental value is 258 GPa,[40] which is consistent with our calculations.

3.2. Energy of formation for point defects

We start the discussions on energetics of defects in MC_x by evaluating the point defect data. There are two possible ways to evaluate the point defect data, namely taking isolated atoms or chemical potentials as the reference, but the trends are the same so we discuss only one the data set with respect to isolated atoms for simplicity reasons. The calculated energy of formation for a single C vacancy and an Al substitution at a C site in TiC_x is 9.916 and 10.140 eV, respectively. As the valence electron concentration increases by substituting Ti with V and further with Cr, these energies of formation decrease to 7.713 and 7.756 eV, respectively, which is a drop by 22.2% and 23.5%, respectively. Similar trends and energy of formation values are obtained for triple vacancies: there is a decrease in the range 21.0–22.9%. Some anomalies from this trend occur when Al is introduced into CrC_x, but this will be discussed below. In order to understand the energy of formation data, we study the electronic structure of these binary carbides. In Fig. 1, the electron density distributions for TiC, VC, and CrC in the (1 1 0) planes are presented. In general, the electronic structure thereof can be described as a mixture of covalent (presence of larger electron concentration between M and C), ionic (charge transfer from M to C), and metallic bonding (uniform background Fermi gas in the whole (1 1 0) plane). As the valence electron concentration increases by substituting Ti in TiC with V and further with Cr, there discernable changes in the bonding can be observed. It is apparent that the electron density located at the C atom decreases. In order to quantify this effect, we have studied the effective charge in these compounds using the Bader decomposition, given in Table 2. The effective charge for C in TiC is −1.672 and increases to −1.298 as the valence electron concentration is increased in the range probed. Since the bulk modulus is increased as the transition metal valence electron concentration is increased, it is reasonable to assume that the ionic character decreases and that the covalent character increases. This notion is also consistent with electronegativity scale difference between the constituents considered. Furthermore, it is known that upon increase in the valence electron concentration by substituting Ti with V and further with Cr more antibonding states are being populated.[41,42] It can be speculated that the introduction of vacancies results in a disruption of antibonding behavior and hence increases the covalent character, as argued above. For instance, the number of states at the Fermi level in VC decreases by 48% upon a C vacancy creation. This change in the bonding character may be used to explain the energy of formation data for point defects (see Table 1), discussed above. The formation energy for vacancies in metals (Al, Pt, Pd, Mo),[28,43] covalent compounds (Si),[43] and ionic (HfO_2, SiO_2),[44] is in the range 1–3, 4, and 5–9 eV, respectively. In covalent crystals, directional bonding may be rearranged upon vacancy creation and local relaxation is observed,[19] while this gives rise to repulsive Coulomb forces in ionic crystals (nearest neighbors of the same charge in the vicinity of a vacancy). This scenario is consistent with the energy of formation data reported in the literature. Here, the formation energy for point defects is decreased as the valence electron concentration is increased, which may be the direct consequence of the decrease in ionic character and the increase in

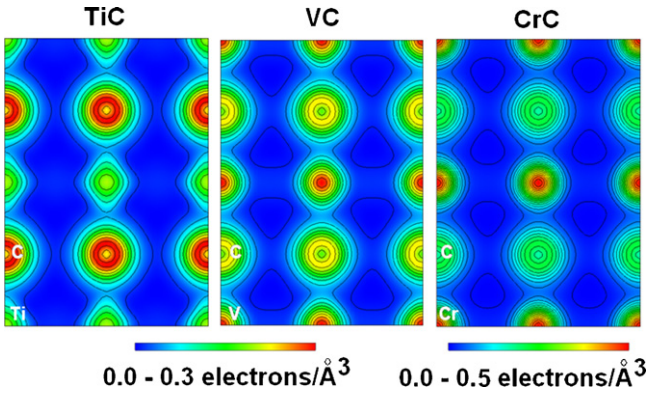

Fig. 1. Electron density distribution for TiC, VC, and CrC in the (1 1 0) plane.

Table 2
Calculated effective charge for MC (M = Ti, V, Cr).

	TiC	VC	CrC
M	1.672	1.518	1.298
C	−1.672	−1.518	−1.298

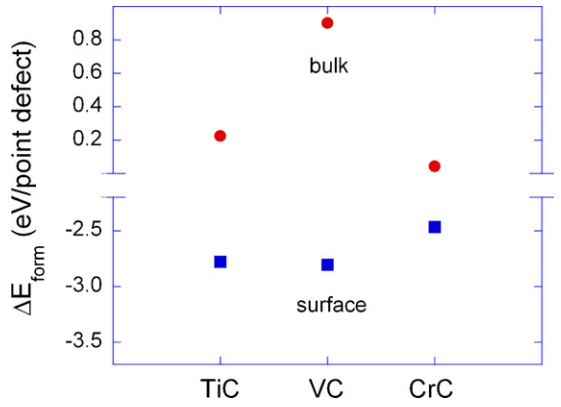

Fig. 2. Difference in the energy of formation (ΔE_{form}) between one Al substitution at a C site and one C vacancy for TiC_x, VC_x, and CrC_x. Data for both bulk and (1 0 0) surface are presented.

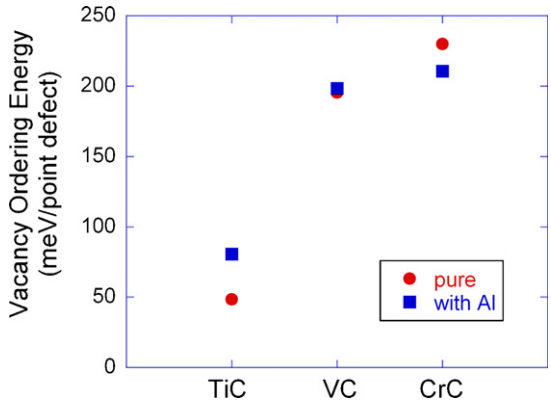

Fig. 3. Vacancy ordering energy for triple point-defects in TiC_x, VC_x, and CrC_x.

the covalent character of the chemical bonding in these binary phases.

Since point defects may randomly be positioned in a crystal, the positions of dispersed triple point defects in the supercells constructed, as described above, should be validated. To investigate the degree of randomness in our supercells, we construct a $2 \times 2 \times 2$ special random structure (SQS) configuration for the triple C vacancy in VC. We use the short range order (SRO) parameter to quantify the degree of randomness in this particular SQS configuration. This is available within the locally self-consistent Green's function software package.[45,46] The SRO parameter for this VC configuration is <0.1 within seven coordination shells. The calculated energy of formation for a triple C vacancy in this SQS configuration differs only 0.6% from the *ad hoc* configuration discussed above. Therefore, our dispersed defects (*ad hoc*) configurations are sufficiently random to describe the energetics of point defects in these binary carbides.

Based on the energetics data presented so far, we can now discuss the likelihood for Al ingress into MC_x lattice. Fig. 2 shows the difference in the energy of formation between one Al substitution at a C site and one C vacancy for TiC_x, VC_x, and CrC_x. The difference between the energy of formation for an Al substitution at a C site and a bulk C vacancy in TiC_x is 0.224 eV, suggesting that Al may be incorporated into the TiC_x lattice, because the magnitude of this energy difference is comparable to the energy required to form metastable cubic $Ti_{1-x}Al_xN$[47] and Cu–Mo[48] by vapor phase condensation. As the valence electron concentration is increased by substituting Ti in TiC_x with V and then with Cr, an increase to 0.900 eV for VC_x is observed and a drop to 0.043 eV, respectively. We speculate that this apparent anomaly for VC_x may be a consequence of the variable valency of V, known for instance to occur in the so-called Magnéli phases.[49] Fig. 2 also shows the corresponding surface data, since the Al/MC_x interface is of importance for the initial stages of Al ingress into MC_x. We have calculated the energetics of a C vacancy and an Al substitution at a vacant C site on the MC_x(1 0 0) surface (see Table 1). The calculated energies of formation for a C vacancy and the Al substitution for TiC_x(1 0 0) are 9.763 and 6.984 eV, respectively (see Table 1). As the valence electron concentration increases by substituting Ti in TiC_x with V and subsequently with Cr, the energies of formation are decreased to 6.835 and 4.369 eV, by 30.0% and 37.4%, respectively. These valence electron concentration induced changes in the energy of formation for these point defects are consistent with the changes observed in bulk as well as the electronic structure changes, discussed above. The general trend is that the energy of formation for a C vacancy on the (1 0 0) surface is smaller than a vacancy within bulk MC_x. An exception is VC_x(1 0 0), but this may again be due to adjustable valency of V.[49] This energy difference can be understood based on the so-called broken-bond model[50,51]; it can be expected that the energy penalty is smaller when less bonds are broken as is the case during formation of a surface vacancy. As Al is introduced into the TiC_x lattice at a C vacancy (1 0 0) surface site, the energy of formation is reduced by 2.779 eV (28.5%), see Fig. 2. Similar energetics is obtained for VC_x and CrC_x (see Fig. 2). These arguments indicate that the incorporation probability of Al at the Al/MC_x interface during bulk synthesis or during vapor phase condensation is high.

3.3. Vacancy ordering and migration energy

Once point defects are present in the MC_x lattice, it remains to be seen if these are mobile enough to eventually form a $M_{n+1}AX_n$ phase. In order to estimate the energetic barriers associated with these dynamic effects, we have calculated the vacancy ordering energy as well as the migration energy (see Table 1). Fig. 3 shows the vacancy ordering energy for triple point defects in TiC_x, VC_x, and CrC_x. Two kinds of vacancy ordering energy were considered: (i) the difference in the energy of formation between three C vacancies ordered along the [1 1 0] direction [(0,0,0), (1/4,1/4,0), (1/2,1/2,0)] and three C vacancies dispersed [(0,0,0), (1/4,3/4,0), (1/4,1/4,1/2)], which is here referred to as pure MC_x, as well as (ii) the difference in the energy of formation between two C vacancies and one Al substitution ordered along the [1 1 0] direction [Al at (0,0,0), vacancies at (1/4,1/4,0), (1/2,1/2,0)] and two C vacancies and one Al substitution dispersed [Al at (0,0,0), vacancies at (1/4,3/4,0), (1/4,1/4,1/2)], which is termed here MC_x with Al. It appears that only 49–81 meV/point defect is required to order the C vacancies in TiC_x. This ordering energy

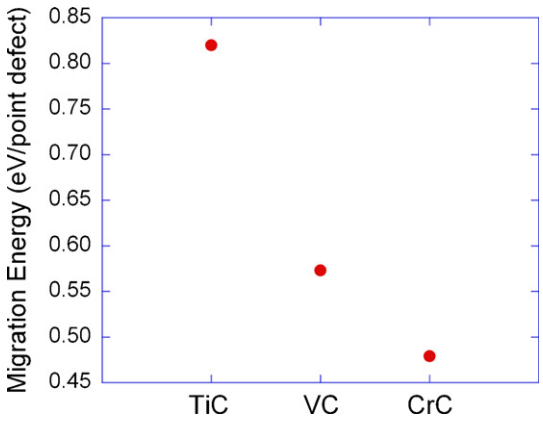

Fig. 4. Migration energy for Al in the [1 1 0] direction for TiC_x, VC_x, and CrC_x.

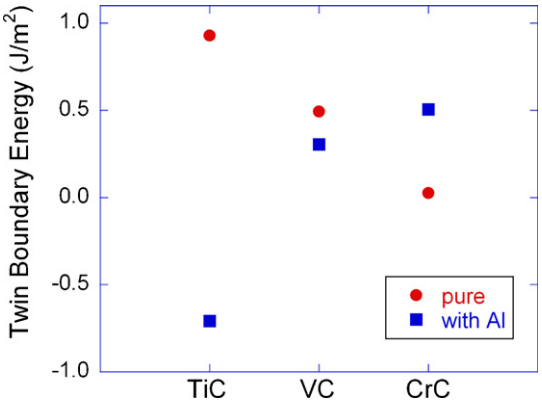

Fig. 5. Twin boundary energy for pure TiC_x, VC_x, and CrC_x, as well as TiC_x, VC_x, and CrC_x with Al at the twin boundary.

increases to 211–230 meV/point defect as the valence electron concentration is increased by substituting Ti in TiC_x with Cr. It is also worth noticing that the ordering energy is not affected by the choice of the reference point (see Table 1). This increase may be due to the change in the bonding nature upon increasing the valence electron concentration; it may be more difficult to order point defects in covalently bonded solids. Nevertheless, these ordering energies are small and may be overcome by magnetron sputtering. For instance, it has been reported that oxygen vacancy ordering occurs in $La_{0.5}Sr_{0.5}CoO_3$ thin films grown by radio-frequency magnetron sputtering.[52] Based on these ordering energies in MC_x, it is reasonable to assume that the formation of Ti_3AlC_2 is accomplished by Al ingress into TiC_x and C vacancy ordering as previously suggested by Riley and Kisi.[15] At temperatures of approximately 1000–1100 °C in vacuum, it has previously been reported that Ti_3SiC_2 rapidly decomposes into TiC_x and Si by egress of Si from the A-site to the crystallite surface and subsequent evaporation.[53] This is in principle a reverse intercalation process. Hence, our intercalation data may also be relevant to describe decomposition and thermal stability. The second dynamic effect to be tackled is the migration energy. Fig. 4 shows the migration energy for Al in the [1 1 0] direction in the TiC_x, VC_x, and CrC_x lattice. As the valence electron concentration in MC_x is increased by substituting Ti with V and further with Cr, the migration energy is decreased from 0.820 to 0.479 eV/point defect, respectively. This may be understood based on the size effect. The radii of ions in 12-coordinated metals of Al, Ti, V, and Cr are 1.43, 1.46, 1.35, and 1.28 Å, respectively.[54] It can be speculated that the migration of particles with large size difference, such as Al in the Cr sublattice, may be enabled. Furthermore, since it is easier to form point defects in CrC_x as compared with VC_x and TiC_x, as discussed above, their mobility may also be larger. Yttria-stabilized zirconia is a well-known ionic conductor and the migration energy of oxygen in this structure was reported to be in the range from 0.20 to 1.40 eV,[55] which is comparable with our data. Based on these data, we suggest that Al moves thermally activated in the MC_x lattice if C vacancies are present. This is consistent with the experimentally reported formation of Ti_3AlC_2 from $TiC_{0.67}$ and molten Al.[15]

3.4. Twin boundary energy

Even if point defects in MC_x are both present and mobile, there is still an additional defect that needs to be considered for the formation of $M_{n+1}AX_n$ by intercalation of Al into MC_x. $M_{n+1}X_n$ building blocks in $M_{n+1}AX_n$ are twinned, which is of course not the case for pure MC_x phases. Fig. 5 shows the twin boundary energy for pure MC_x and MC_x with Al at the twin boundary. Here, *M* elements at the twin boundary are substituted with Al following the experimental observations on twinning.[20] As the valence electron concentration in MC_x is increased by substituting Ti with V and further with Cr, the twin boundary energy is decreased from 0.929 to 0.026 J/m^2 for pure MC_x and increased from −0.709 to 0.505 J/m^2 for MC_x with Al at the twin boundary. From the latter data the spontaneous formation of twins can be inferred, which is consistent with previously calculated twin boundary energies and stacking fault energies in TiC_x[20,56] as well as experimental observations.[20] In order to understand these trends, we study the electronic structure of these twinned crystals. Fig. 6 shows the electron density distribution in the (1 1 $\bar{2}$ 0) plane for twinned MC_x and MC_x with Al at the twin boundary. Similar to the defect-free *M*C phases (see Fig. 1), the electronic structure can be described as a mixture of

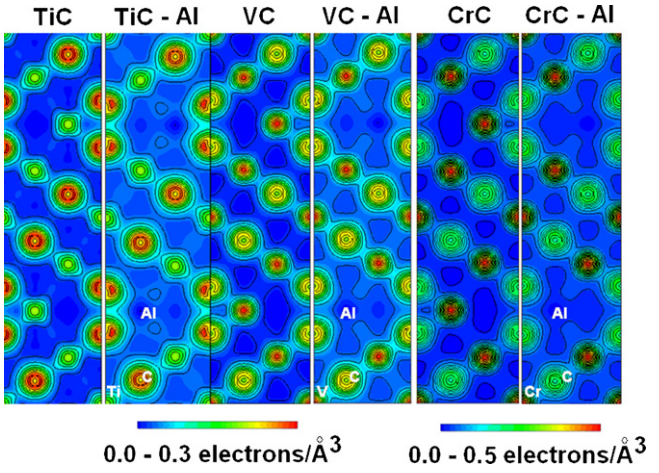

Fig. 6. Electron density distribution in the (1 1 $\bar{2}$ 0) plane for twinned TiC_x, VC_x, and CrC_x, as well as twinned TiC_x, VC_x, and CrC_x with Al at the twin boundary.

covalent, ionic, and metallic bonding. As the valence electron concentration is increased by substituting Ti in TiC_x with V and further with Cr, there are considerable changes in the bonding nature. It is observed that the electron density located spherically around the C atom decreases, while the electron density between the *M* and C atoms is increased, which in turn indicates that the covalent character is increased. This is consistent with the increase in bulk modulus, see Table 1. Another noticeable change is that Al disrupts the bonding more in CrC_x as compared with VC_x and TiC_x. By comparing the electron density distributions around *M* and Al in MC_x, it may be deduced that the bonding character of Al is still to some extent similar to Ti in TiC_x due to conservation of the 4-fold symmetry. As Ti is substituted by V and Cr, the bonding character of Al is no longer similar to *M* in MC_x, since the local symmetry is broken on the electronic level and there is a larger difference in the number of valence electrons. This may also be related to the energy of formation anomaly regarding Al substitution at the C site in CrC_x, discussed above. Hence, twinning in MC_x is expected to be energetically favorable as the valence electron concentration is increased since the bonding becomes less ionic (ionic crystals normally deform plastically to a lesser extent). Opposite occurs for the twinned MC_x with Al at the twin boundary. The overall bonding is disturbed (local symmetry breaking on the electronic level) by introduction of Al into MC_x as the valence electron density increases so that twinning is expected to be energetically less favorable. It may be speculated that in TiC_x twinning is Al mediated, while in VC_x and CrC_x twins may form before the ingress of molten Al. Therefore, it is expected based on the twin boundary energy as well as the point defect energetics studied here that rapid intercalation of MC_x phases is possible. Based on these results, the low temperature synthesis of VC_x and CrC_x containing $M_{n+1}AX_n$ phases appears realizable.

4. Conclusions

Density functional theory was used to study the energetics of point defects and twins in MC_x ($x<1$, M = Ti, V, Cr). We probed C vacancies, Al substitution at a C site, ordering of C vacancies with and without Al, migration of Al in the MC_x lattice, as well as twin boundary energy with and without Al. Our objective is to contribute towards understanding the underlying atomic mechanisms enabling the Al intercalation into MC_x. As the valence electron concentration is increased by substituting Ti in TiC_x with V and further with Cr, the energy of formation for both C vacancies and Al substitutions at C sites is decreased by up to 24%. This may be understood based on the electronic structure by studying the electron density distribution and the effective charge by Bader decomposition. Upon increasing the valence electron concentration, the bonding becomes less ionic and more covalent. In covalent crystals, directional bonding may be rearranged and local relaxation is observed upon vacancy creation, while this gives rise to repulsive Coulomb forces in ionic crystals, and hence the energy of formation is expected to decrease as the valence electron concentration of *M* is increased. The difference between the energy of formation for an Al substitution at a C site and a bulk C vacancy in MC_x, the migration energy, as well as the point defect ordering energy may be overcome during vapor phase condensation. Surface effects were also considered: the energy of formation for Al on MC_x(1 0 0) at a vacant surface C site is >2 eV smaller than in the case of the C surface vacancy, indicating that Al is likely to be incorporated. As the valence electron concentration of *M* in MC_x is increased by substituting Ti with V and further with Cr, the twin boundary energy decreases from 0.929 to 0.026 J/m^2 for pure MC_x and increases from −0.709 to 0.505 J/m^2 for MC_x with Al at the twin boundary. This can again be explained using the electronic structure. Based on these energetics considerations, we suggest that intercalation of Al into MC_x is feasible during processing at low temperatures.

Acknowledgements

We acknowledge financial support from DFG (Schn 735/15-1, “Adaptive Oberflächen für Hochtemperatur-Anwendungen”).

References

1. Gozzi, D., Guzzardi, G., Montozzi, M. and Cignini, P. L., Kinetics of high temperature oxidation of refractory carbides. *Solid State Ionics*, 1997, **101–103**, 1243–1250.
2. Hugosson, H. W., Jansson, U., Johansson, B. and Eriksson, O., Restricting dislocation movement in transition metal carbides by phase stability tuning. *Science*, 2001, **293**, 2434–2437.
3. Jhi, S.-H., Ihm, J., Louie, S. G. and Cohen, M. L., Electronic mechanism of hardness enhancement in transition-metal carbonitrides. *Nature*, 1999, **399**(6732), 132–134.
4. Wu, Z., Chen, X.-J., Struzhkin, V. V. and Cohen, R. E., Trends in elasticity and electronic structure of transition-metal nitrides and carbides from first principles. *Phys. Rev. B*, 2005, **71**(21), 214103.
5. Radosevich, L. G. and Williams, W. S., Thermal conductivity of transition metal carbides. *J. Am. Ceram. Soc.*, 1970, **53**(1), 30–33.
6. Chien, F. R., Ning, X. J. and Heuer, A. H., Slip systems and dislocation emission from crack tips in single crystal TiC at low temperatures. *Acta Mater.*, 1996, **44**(6), 2265–2283.
7. Gee, M. G., Roebuck, B., Lindahl, P. and Andren, H.-O., Constituent phase nanoindentation of WC/Co and Ti(C,N) hard metals. *Mater. Sci. Eng. A*, 1996, **209**(1–2), 128–136.
8. Menig, R., Meyers, M. H., Meyers, M. A. and Vecchio, K. S., Quasi-static and dynamic mechanical response of Strombus gigas (conch) shells. *Mater. Sci. Eng. A*, 2001, **297**(1–2), 203–211.
9. Raabe, D., Sachs, C. and Romano, P., The crustacean exoskeleton as an example of a structurally and mechanically graded biological nanocomposite material. *Acta Mater.*, 2005, **53**(15), 4281–4292.
10. Barsoum, M. W., The $M_{n+1}AX_n$ phases: a new class of solids; thermodynamically stable nanolaminates. *Prog. Solid St. Chem.*, 2000, **28**(1–4), 201–281.
11. Music, D. and Schneider, J. M., The correlation between the electronic structure and elastic properties of nanolaminates. *JOM*, 2007, **59**(7), 60–64.
12. Lin, Z. J., Li, M. S. and Zhou, Y. C., TEM investigations on layered ternary ceramics. *J. Mater. Sci. Technol.*, 2007, **23**(2), 145–165.
13. Boehm, H.-P., Setton, R. and Stumpp, E., Nomenclature and terminology of graphite-intercalation compounds (IUPAC recommendations 1994). *Pure Appl. Chem.*, 1994, **66**(9), 1893–1901.
14. Katinonkul, W. and Lerner, M. M., Graphite intercalation compounds with large fluoroanions. *J. Fluorine Chem.*, 2007, **128**(4), 332–335.
15. Riley, D. P. and Kisi, E. H., The design of crystalline precursors for the synthesis of $M_{n+1}AX_n$ phases and their application to Ti_3AlC_2. *J. Am. Ceram. Soc.*, 2007, **90**(7), 2231–2235.
16. Zhou, Y. C. and Sun, Z. M., Crystallographic relations between Ti_3SiC_2 and TiC. *Mater. Res. Innovat.*, 2000, **3**(5), 286–291.

17. Wang, X. H. and Zhou, Y. C., Stability and selective oxidation of aluminum in nano-laminate Ti_3AlC_2 upon heating in argon. *Chem. Mater.*, 2003, **15**(190), 3716–3720.
18. Kooi, B. J., Kabel, M., Kloosterman, A. B. and de Hossan, J. Th. M., Reaction layers around SiC particles in Ti: an electron microscopy study. *Acta Mater.*, 1999, **47**(20), 3105–3116.
19. Music, D., Riley, D. P. and Schneider, J. M., Energetics of point defects in TiC. *J. Eur. Ceram. Soc.*, 2009, **29**(4), 773–777.
20. Yu, R., He, L. L. and He, H. Q., Effects of Si and Al on twin boundary energy of TiC. *Acta Mater.*, 2003, **51**(9), 2477–2484.
21. Hohenberg, P. and Kohn, W., Inhomogeneous electron gas. *Phys. Rev.*, 1964, **136**(3B), B864–B871.
22. Kresse, G. and Joubert, D., From ultrasoft pseudopotentials to the projector augmented-wave method. *Phys. Rev. B*, 1999, **59**(3), 1758–1775.
23. Blöchl, P. E., Projector augmented-wave method. *Phys. Rev. B*, 1994, **50**(24), 17953–17979.
24. Monkhorst, H. J. and Pack, J. D., Special points for Brillouin-zone integrations. *Phys. Rev. B*, 1976, **13**(12), 5188–5192.
25. Wilhelmsson, O., Rasander, M., Carlsson, M., Lewin, E., Sanyal, B., Wiklund, U., Eriksson, O. and Jansson, U., Design of nanocomposite low-friction coatings. *Adv. Funct. Mater.*, 2007, **17**(10), 1611–1616.
26. Wilhelmsson, O., Palmquist, J. P., Lewin, E., Emmerlich, J., Eklund, P., Persson, P. O. Å., Högberg, H., Li, S., Ahuja, R., Eriksson, O., Hultman, L. and Jansson, U., Deposition and characterization of ternary thin films with the Ti–Al–C system by DC magnetron sputtering. *J. Cryst. Growth*, 2006, **291**(1), 290–300.
27. Birch, F., Finite strain isotherm and velocities for single-crystal and polycrystalline NaCl at high-pressures and 300-degree-K. *J. Geophys. Res.*, 1978, **83**(NB3), 1257–1268.
28. Mattsson, T. R. and Mattsson, A. E., Calculating the vacancy formation energy in metals: Pt, Pd, and Mo. *Phys. Rev. B*, 2002, **66**(21), 214110.
29. Choi, M., Oba, F. and Tanaka, I., First-principle study of native defects and lanthanum impurities in $NaTaO_3$. *Phys. Rev. B*, 2008, **78**(1), 014115.
30. Van de Walle, C. G. and Neugebauer, J., First-principles calculations for defects and impurities: applications to III-nitrides. *J. Appl. Phys.*, 2004, **95**(8), 3851.
31. Momma, K. and Izumi, F., VESTA: a three-dimensional visualization system for electronic and structural analysis. *J. Appl. Cryst.*, 2008, **41**, 653–658.
32. Allred, A. L. and Rochow, E. G., A scale of electronegativity based on electrostatic force. *J. Inorg. Nucl. Chem.*, 1958, **5**(4), 264–268.
33. Henkelman, G., Arnaldsson, A. and Jónsson, H., A fast and robust algorithm for Bader decomposition of charge density. *Comp. Mater. Sci.*, 2006, **36**(3), 354–360.
34. Sanville, E., Kenny, S. D., Smith, R. and Henkelman, G., Improved grid-based algorithm for Bader charge allocation. *J. Comp. Chem.*, 2007, **28**(5), 899–908.
35. Shimada, S., Watanabe, J., Kodaira, K. and Matsushita, T., Flux growth and characterization of TiC crystals. *J. Mater. Sci.*, 1989, **24**(7), 2513–2515.
36. Pflüger, J., Fink, J., Weber, W., Bohnen, K.-P. and Crecelius, G., Dielectric-properties of TiC_x, TiN_x, VC_x, and VN_x from 1.5 to 40 eV determined by electron-energy-loss spectroscopy. *Phys. Rev. B*, 1984, **30**(3), 1155–1163.
37. Jian, W., Xiangyi, C., Nan, Y. and Zhengzhi, F., Formation of NaCl-type Cr carbide by carbon ion implantation. *Appl. Phys. A*, 1993, **56**, 307–309.
38. Dodd, S. P., Cankurtaran, M. and James, B., Ultrasonic determination of the elastic and nonlinear acoustic properties of transition-metal carbide ceramics: TiC and TaC. *J. Mater. Sci.*, 2003, **38**(6), 1107–1115.
39. Hugosson, H. W., Korzhavyi, P., Jansson, U., Johansson, B. and Eriksson, O., Phase stabilities and structural relaxations in substoichiometric TiC_{1-x}. *Phys. Rev. B*, 2001, **63**(16), 165116.
40. Liermann, H. P., Singh, A. K., Manoun, B., Saxena, S. K., Prakapenka, V. B. and Shen, G., Compression behavior of $VC_{0.85}$ up to 53 GPa. *Int. J. Ref. Met. Hard Mater.*, 2004, **22**(2–3), 129–132.
41. Häglund, J., Grimvall, G., Jarlborg, T. and Fernández Guillerment, A., Band structure and cohesive properties of 3d-transition-metal carbides and nitrides with the NaCl-type structure. *Phys. Rev. B*, 1991, **43**(18), 14400–14408.
42. Grechnev, A., Ahuja, R. and Eriksson, E., Balanced crystal orbital overlap population—a tool for analyzing chemical bonds in solids. *J. Phys.: Condens. Matter*, 2003, **15**(45), 7751–7761.
43. Armiento, R. and Mattsson, A. E., Functional designed to include surface effects in self-consistent density functional theory. *Phys. Rev. B*, 2005, **72**(8), 085108.
44. Scopel, W. L., da Silva, A. J. R., Orellana, W. and Fazzio, A., Comparative study of defect energetics in HfO_2 and SiO_2. *Appl. Phys. Lett.*, 2004, **84**(9), 1492–1494.
45. Abrikosov, I. A., Niklasson, A. M. N., Simak, S. I., Johansson, B., Ruban, A. V. and Skriver, H. L., Order-N Green's function technique for local environment effects in alloys. *Phys. Rev. Lett.*, 1996, **76**(22), 4203–4206.
46. Abrikosov, I. A., Simak, S. I., Johansson, B., Ruban, A. V. and Skriver, H. L., Locally self-consistent Green's function approach to the electronic structure problem. *Phys. Rev. B*, 1997, **56**(15), 9319–9334.
47. Mayrhofer, P. H., Music, D. and Schneider, J. M., Influence of the Al distribution on the structure, elastic properties, and phase stability of supersaturated $Ti_{1-x}Al_xN$. *J. Appl. Phys.*, 2006, **100**(9), 094906.
48. Gong, H. R., Kong, L. T. and Liu, B. X., Metastability of an immiscible Cu–Mo system calculated from first-principles and a derived n-body potential. *Phys. Rev. B*, 2004, **69**(2), 024202.
49. Katzke, H., Tolédano, P. and Depmeier, W., Theory of morphotropic transformations in vanadium oxides. *Phys. Rev. B*, 2003, **68**(2), 024109.
50. Bragg, W. L. and Williams, E. J., The effect of thermal agitation on atomic arrangement in alloys. *Proc. Roy. Soc. London*, 1934, **145**, 699–730.
51. Becker, R., *Ann. Phys.*, 1938, **32**, 128–140.
52. Klenov, D. O., Donner, W., Chen, L., Jacobson, A. J. and Stemmer, S., Composition control of radio-frequency magnetron sputter-deposited $La_{0.5}Sr_{0.5}CoO_3$-partial derivative thin films. *J. Mater. Res.*, 2003, **18**(1), 188–194.
53. Emmerlich, J., Music, D., Eklund, P., Wilhelmsson, O., Jansson, U., Schneider, J. M., Högberg, H. and Hultman, L., Thermal stability of Ti_3SiC_2 thin films. *Acta Mater.*, 2007, **55**(4), 1479–1488.
54. Kittel, C., *Introduction to Solid State Physics*. John Wiley & Sons, Inc., New York, 1996, p. 78.
55. Pornprasertsuk, R., Ramanarayanan, P., Musgrave, C. B. and Prinz, F. B., Predicting ionic conductivity of solid oxide fuel cell electrolyte from first principles. *J. Appl. Phys.*, 2005, **98**(10), 103513.
56. Harris, R. M. and Bristowe, P. D., Computer modeling of slip in TiC. *Philos. Mag. A*, 1999, **79**(3), 705–721.